ISSN (Print) 1226-1750
ISSN (Online) 2233-6656
Journal of Magnetics 18(1), 9-13 (2013) http://dx.doi.org/10.4283/JMAG.2013.18.1.009

The Effect of Crystal and Non-Crystal Structures on Shielding Material Behaviour Under A.C. Field Excitations

Nazaruddin Abd Rahman[1]* and Wan Nor liza Mahadi[2]

[1]*Electrical Power Department, College of Engineering, Universiti Tenaga Nasional 43009 Kajang, Selangor*
[2]*Electrical Engineering Department., Faculty of Engineering, University of Malaya, 50830 Kuala Lumpur*

(Received 29 October 2012, Received in final form 12 March 2013, Accepted 12 March 2013)

Shielding effects in conductive and magnetic materials were investigated as a function of properties, thickness and diameter. In this work, evaluations on passive conductive and magnetic shield specimens were achieved through experimentation set-up using 50 Hz single and three phase induction field sources. Analysis on material microstructure properties and characteristics of shielding specimens were performed with the use of vibrating sample magnetometer (VSM) and field emission scanning electron microscopy (FESEM). An induction field at 136 μT of single phase system and 50 μT of three phase systems were observed to the shield specimens with the thickness ranged of 0.2 mm to 0.4 mm. It is observed that shield specimen efficiency becomes inversely proportionate to the increment of induction fields. The decrease was attributed to the surface structure texture which relates to the crystallization and non-crystallization geometrical effects.

Keywords : shielding efficiency, magnetic field, shield materials, crystallization

1. Introduction

Magnetic field shielding is one of the most important solutions in ensuring public safety which are exposed to high magnetic field emission. It is used as mitigation efforts in safeguarding the emission impact to the surrounding area. In the earlier stage shielding research were embarked by studying shield geometrical effects with its exposure behaviour response [1-3]. Further on, the progresses on shielding works were advanced with the development of complete shielding theory as an alternative choice to the experimentation work [4]. Shielding technology draws one important aspect in mitigating the electromagnetic problem which is the integrity of shield material selection. These materials are usually limited to the element of conductive and magnetic materials. Shield effects and material performances were closely monitored in the applications of Ferrum-Silicon Non-Oriented (Fe-Si (NO)), Ferrum-Silicon Grain Oriented (Fe-Si (GO)) and Ferrum-Carbon (Fe-C) as shown in the study conducted by Bottauscio *et al.* [5]. The materials had indicated field reductions with almost 66.7% for Fe-Si GO, 58.3% for Fe-Si NO and 50.0% for low carbon steel. However, permeability values were not revealed in the study.

There were also studies that correlate shield material performances with geometrical shield designs. This was performed by Du *et al.* [6] where comparisons of conductive material such as Aluminum (Al) and magnetic materials of Fe-Si and Mu-metal were conducted in thickness of 0.5 mm and 0.36 mm respectively. Experimentation in a flat sheet shielding design indicates shielding effectiveness of Al, Fe-Si and Mu-metal were significantly reducing the fields by 0.7, 0.5 and 0.02 respectively. These results were apparently within the approximated relative permeability value properties of 1, 1100 and 3500. Comprehensive results were observed by Beltran and Fuster [7] where shielding performances of various materials were studied in a single and double layer screening experimentations. Field reduction percentages are reciprocated higher in two layers as compared to single layer shields. Previous work thus indicates that both conductive and magnetic materials had handful strength to perform emission screens. It is therefore necessary to further examine the effects of crystallization in determine shielding performances among these materials. This study observes and characterizes the types of materials element that leads to shielding performances which include factors such as thickness and materials properties.

*Corresponding author: Tel: +603-8921-2020
Fax: +603-8928-7166, e-mail: nazaruddin@uniten.edu.my

Table 1. Types of shield materials used in the study including thickness values.

Shield Materials	Material Grade	Thickness, t (mm)
Fe-Si GO	M5 (0.3)	0.3
Fe-Si NGO	50H (470)	0.26
Al	AA11000-H14	0.3
Fe-C-Zn (EG)	G3313	0.4
Fe-Zn (GI)	G3302	0.3

2. Experimental Method

The initial set up for experimental work involves preparations of shield materials as shown in Table 1. The work requires shield materials to be designed according to its specific geometry sizes that suited with field measurement systems. Process for shaping the shield material involves two types of geometry design which comes in rectangular and cylindrical shape specimens. Each size of shielding specimens contains a cross-sectional of 90 × 90 mm and 1220 mm respectively. The use of vibrating sample magnetometer (VSM) helps the identification process of magnetic properties. The results were analysed with hysteresis graphs by characterizing the behaviour of conductive and magnetic elements in the shield specimens. Field induction test in rectangular shields were exposed in a magnetize condition of 415 V three phase electric system while in cylindrical shields field exposure were induced from 240 V single phase electric condition. Both field test systems produced a maximum power of 9 kVA and 0.3 kVA respectively. With similar parameters the maximum field fluxes produced in the systems were encountered reach to the level of 50 μT and 136 μT respectively. Other requirements such as specimen orientations in the test rig were determined based on the types of applied field exposures. In this case, each specimen is positioning in a vertical and horizontal direction. The morphological analysis applied to the shield specimens helps in correlating shield performances behaviour. The correlations were examined by capturing a microscopic layer view with field emission scanning electron microscopic (FESEM). The schematic diagram of overall experimental set up is shown in Fig. 1.

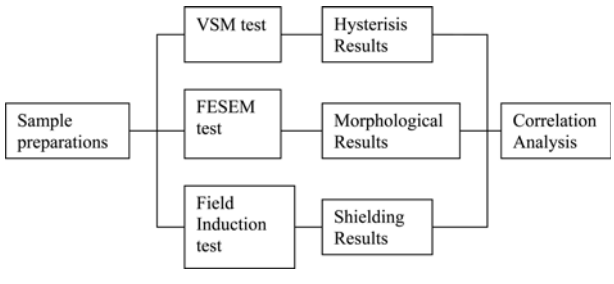

Fig. 1. Schematic diagram of experimental set up.

3. Results and Discussion

A hysteresis graph for all the specimens were obtained as given in Fig. 2. The results represent five types of shield materials which consist of grain oriented silicon iron (Fe-Si GO), non-grain oriented silicon iron (Fe-Si NGO), galvanized iron (Fe-Zn) and electro-galvanized steel (Fe-C-Zn). The VSM test specimens were prepared by cutting each material specimen into 20 × 20 mm. Hysteresis graphs obtained in the evaluations were used to characterize and differentiate properties of magnetic and conductive elements found in the shield specimens. It represents descending hysteresis curves in which to characterize the materials, leaving off the ascending curves and point of origin coordinates. All curve points that cut through at y-axis while x = 0 represent saturation remanence while points cut at x-axis while y = 0 represent coercivity remanence. It is observed that Fe-Si GO, Fe-Si NGO and Fe-C-Zn (EG) were classified as perfect magnetic hysteresis curves of ferromagnetic types while Al shown mild characteristic of paramagnetic types and so as to Fe-Zn (GI) which attributes to diamagnetic types that signified the material as purely conductive. Results in magnetic materials were supported with magnetic saturation values in which fallen within levels from 200 emu/g to 175 emu/g of material specimens.

The correlations of material specimens with previous results were further elaborated with the use of field emission scanning electron microscope (FESEM). This is carried out by characterizing the physical material texture

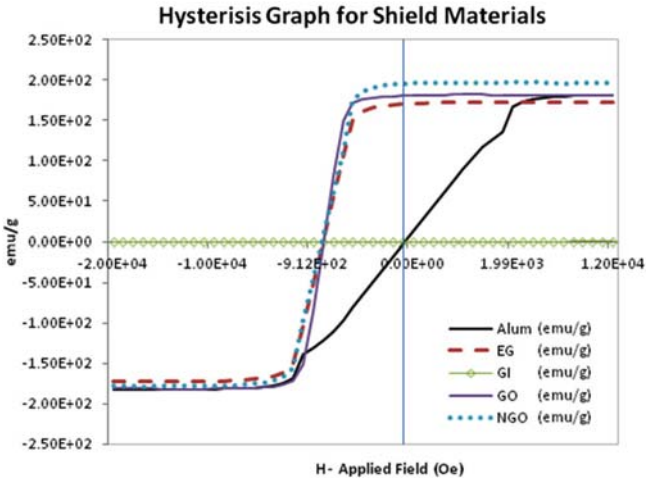

Fig. 2. (Color online) Hysterisis graph that shows the characteristics of each material specimens.

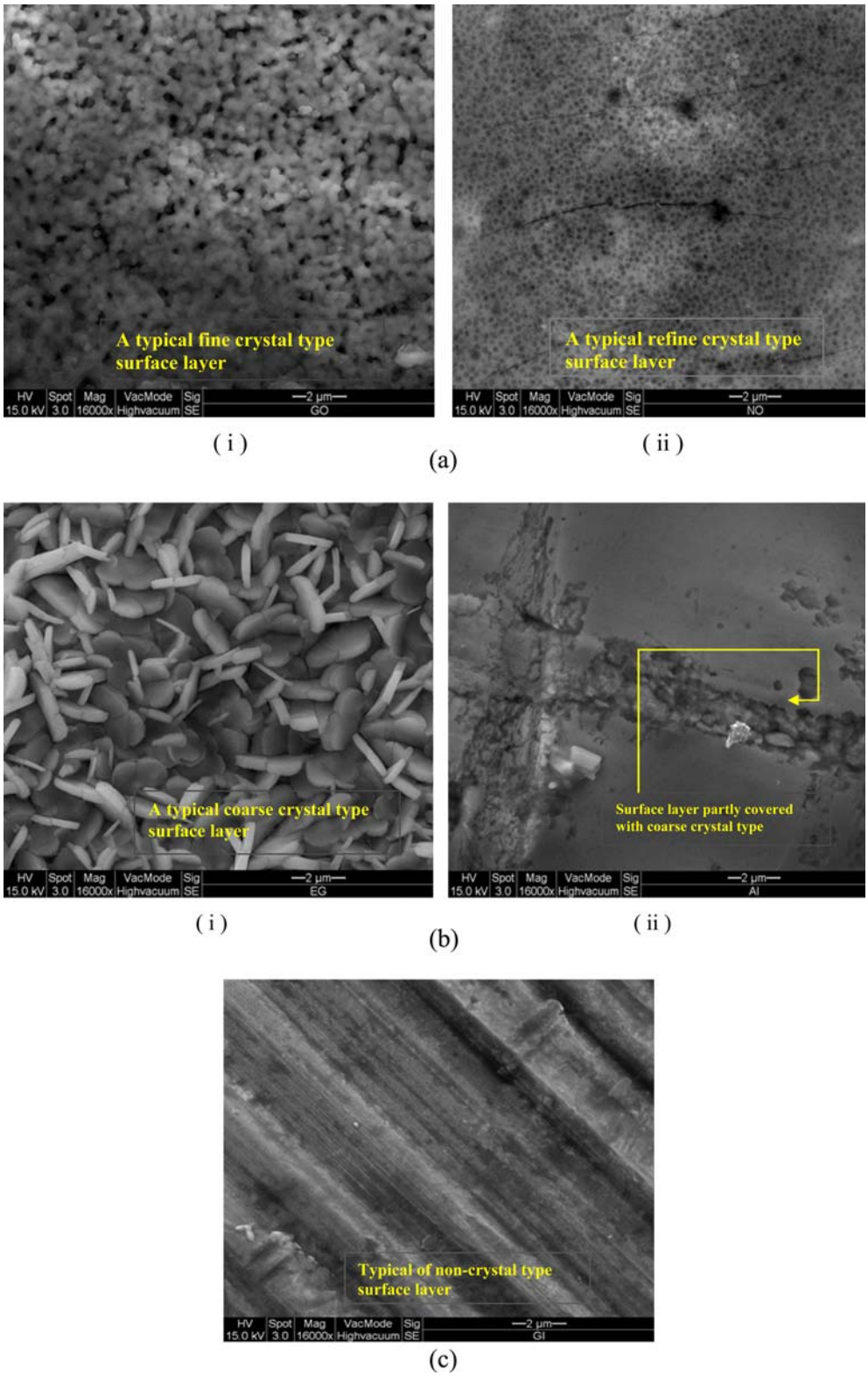

Fig. 3. (Color online) (a) (i) Fe-Si GO and (ii) Fe-Si NGO microscopic view at 2 μm thickness layer. (b) (i) Fe-C-Zn (EG) and (ii) Al microscopic view at 2 μm thickness layer. (c) Fe-Zn (GI) microscopic view at 2 μm thickness layer.

with the conductive and magnetic elements. Analysis work on material specimens were scanned at 2 μm thickness layers which directly signified the result performance shown in VSM. The microstructure layers of Fe-Si GO,

Fe-Si NGO and Fe-C-Zn exhibit a formation of crystal structure within the entire region as shown in Fig. 3(a) (i-ii) and (b) (i). It indicates that Fe-Si NGO distinguished a very fine crystal structure as compared to Fe-Si GO which had slightly larger in geometrical size. These materials were also fairly different from Fe-C-Zn whereby on this material the solid structure was a formation of coarse crystal type surface layer. A contrary finding was found in Al and Fe-Zn of Fig. 3(b) (ii) and (c) whereby on this evaluation the formations of crystal structure were undetermined in Al and completely insignificant in Fe-Zn materials. These two resultants described on the different structure of magnetic and conductive elements in the test specimens. It also relates the presence of crystal structure at the microscopic layers with magnetic saturation levels through various crystal geometrical sizes within the specimens [11].

The formation of crystal structures also indicating the existence of relative permeability, μ_r values while for non-crystal structures the parameter appeared to be insignificant. Relative permeability values obtained through VSM systems also revealed Fe-Si GO and Fe-Si NGO with 1500 and 500 respectively while for Fe-C-Zn is within 200 [8]. However, material specimens for non-crystal structures such as Al and Fe-Zn had resorting in higher relative conductivity values, σ_r with each 3.8×10^7 S/m and 1.67×10^7 S/m while other materials were in the range of lower conductivity values. These two intrinsic properties were denoted as a function of shield effects in determining field reductions. The mechanism shows that shield effects in materials with relative permeability values absorbing the field fluxes through susceptibility process while materials with high relative conductivity spurs the eddy current to perform shield effects [9, 10].

Result in Fig. 4 shows a contribution of all shield specimens in giving respond towards shield effects within the electromagnetic induction of single and three phase systems. The field induction test which measured at 50 μT and 136 μT were exposed to the verified shield specimens of conductive and magnetic elements. Analysis data were made by comparing results given in both conditions. The result shows that at low field exposure, shield effects are relatively high with above than 50% field reduction were obtained from shield materials of Fe-Si GO, Fe-Si NGO and Fe-C-Zn (EG). Other materials which performed less than 50% reductions were Al and Fe-Zn (GI). As the field exposure increases to 136 μT, the shielding strength for Fe-Si GO and Fe-Si NGO were seen dropped and encountered shielding losses with breakdown losses percentage to 39.6% and 38.4% respectively. The highest breakdown losses were seen produced by Fe-C-Zn (EG)

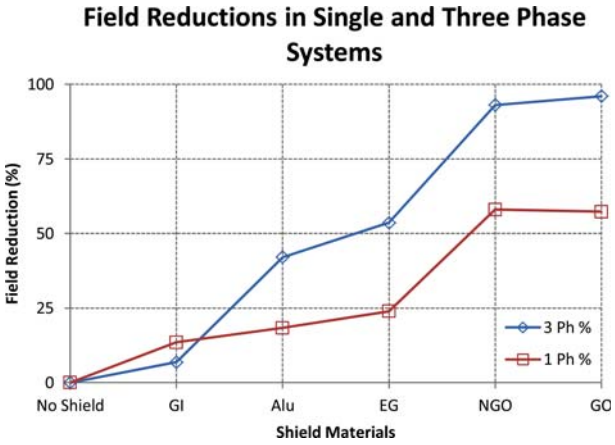

Fig. 4. (Color online) Correlation results of shielding materials with respect to field reductions.

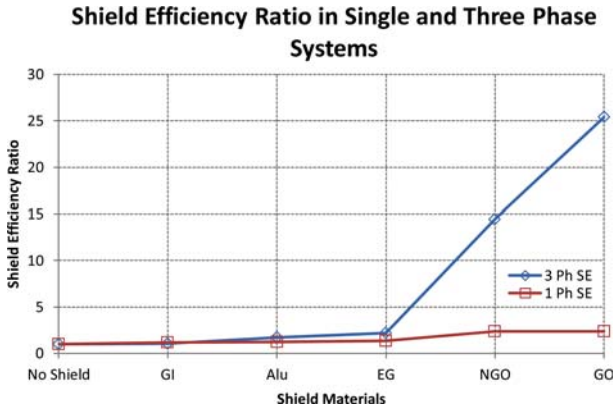

Fig. 5. (Color online) Correlation results of shielding materials with respect to shielding efficiency.

with 55.2% dropped while conductive materials such as Al losing its shield strength to 43%. However, Fe-Zn (GI) shows an increment of shielding with 45.2% improved shield strength in higher field conditions as compared with lower conditions.

The next line of evaluation parameters relates material shield strength with effective shield material resultant as given in Fig. 5. Shielding efficiency is calculated based on its ratio of undisturbed shield condition with shielded condition. The resultants had indicated that Fe-Si GO and Fe-Si NGO materials performed good effective shielding when exposed at 50 μT with higher field reductions of 96.06% and 93.06% respectively. Other choices of moderate shield effects were given by Fe-C-Zn (EG) material with field reduction of 53.60% while Al 42.08%. The poorest field reduction was given by Fe-Zn (GI) material which produced only 6.88%. However, as the exposure range increases to 136 μT most material specimens were performed at low efficient level due to losses in shield

strength. One of the reasons of poor performances was due to its low conductivity value in giving adequate energy to generate eddy current effects. A similar case went to happen in perfect magnetic materials whereby the materials were losing its shield strength when magnetization force had exceeded from its saturation level boundary. In order to increase its efficiency, material design and optimization is recommended for technical consideration.

4. Conclusions

The effects of crystal and non-crystallization microstructures were investigated in conjunction to its shielding performances. This experiment proves the important role of surface structure in determining shield efficiency based on the following observations below:

1. Analysis conducted with FESEM shows two characteristics of crystal and non-crystal microstructure behaviours which differentiate the two structure layers of conductive materials represented by Fe-Zn (GI) and Al, while magnetic materials were represented by Fe-Si GO, Fe-Si NGO and Fe-C-Zn (EG). It shows that materials with crystal microstructure perform better electromagnetic shielding performance as compared with non-crystal structures that produced very minimal effects.

2. Crystal microstructure is also significant with saturation of magnetization in magnetic shielding materials which inversely proportionate to the field intensity as shown by Fe-Si GO, Fe-Si NGO and Fe-C-Zn. This means constant increment of relative permeability value shall indicate an enhancement of magnetic saturation levels thus intensify the rate of shielding effects. So as to perfect conductive material which is non-crystal type whereby the material works better in shielding which is having higher electric conductivity values as shown by Fe-Zn and Al.

3. Efficiency results had indicated that thickness parameter is so significant with materials in Fe-Zn, Al and Fe-C-Zn but not significant with Fe-Si GO and Fe-Si NGO. This clearly explained that the shield effects were a function of skin depth and relative conductivity in conductive materials while magnetic materials were only dependable to the function of relative permeability values.

References

[1] D. A. Miller and J. E. Bridges, IEEE Trans. Elect. Comp. **8**, 4 (1966).
[2] A. J. Mager, IEEE Trans. Magn. **6**, 1 (1970).
[3] R. B. Schulz, IEEE Trans. Elect. Comp. **10**, 1 (1968).
[4] R. B. Schulz, V. C. Plantz, and D. R. Brush, IEEE Trans. Comp. **30**, 3 (1988).
[5] O. Bottauscio, M. Chiampi, D. Chiarabaglio, and M. Zucca, J. Magn. Magn. Mater. **215**, 216 (2000).
[6] Y. Du, T. C. Cheng, and A. S. Farag, IEEE Trans. Elect. Comp. **38**, 3 (1996).
[7] H. Beltran, and V. Fuster, Elect. Pow. Syst. Res. **78**, 1080 (2008).
[8] R. J. W. Donald, A handbook on Electromagnetic Shielding Materials and Performance, Don White Consultant, Inc., Virginia (1980) pp. 14-17.
[9] P. Moreno and R. G. Olsen, IEEE Trans. Power Del. **25**, 4 (2010).
[10] B. A. Clairmont and R. J. Lordan, IEEE Trans. Power Del. **14**, 4 (1999).
[11] B. Ahmadi, H. Chazal, T. Waeckerle, and J. Roudet, IEEE Trans. Magn. **46**, 12 (2010).